

## Production and Crystallization Behavior of an Iron Rich Glass–Ceramic Prepared by Ironmaking and Steelmaking Wastes

S. Ghasemi <sup>1\*</sup>, A. Shafyei <sup>2</sup>

<sup>1</sup> Department of Metallurgy and Materials Engineering, Hamedan University of Technology, Hamedan 65155- 579, Iran

<sup>2</sup> Department of Materials Engineering, Isfahan University of Technology (IUT), Isfahan 84156- 83111, Iran

### Abstract

Using wastes as starting raw materials is a common method to reduce the production costs and the environmental pollution problems arising from such wastes. In this study the production and crystallization behavior of an iron rich glass prepared by iron and steel making wastes has been investigated. The raw materials used, were the blast furnace slag, the blast furnace dust, converter slag and sludge, and agglomeration sludge. The glass was prepared by melting the proper amounts of raw materials at 1400 °C and devitrification of the glass followed by appropriate heat treatment at 850 °C. The as cast glass was characterized by differential thermal analysis, X-ray diffraction to assess the structural evolutions and scanning electron microscopy. The results showed that after the crystallization of the base glass at 850 °C, the major crystalline phase was diopside and it nucleated heterogeneously on colloidal iron particles which were present in the base glass. In fact, the ceramic phases surrounded the metallic iron particles confirmed that these metallic particles could be suitable heterogeneous sites for nucleation of crystalline phases.

**Keywords:** Glass-Ceramics; Crystallization; Iron and steel making wastes.

### 1. Introduction

Glass ceramics are polycrystalline solids prepared by the controlled crystallization of glasses. Crystallization is accomplished by subjecting suitable glasses to a carefully regulated heat treatment schedule which results in the nucleation and growth of fine and equally distributed crystal phases within the glassy matrix. Glass-ceramics combine the properties of glasses such as high temperature formability with many of the advantageous properties of ceramics. They are finding increasing application by virtue of their strength, high chemical durability, hardness, and abrasion resistance <sup>1)</sup>.

The main constituents of glass-ceramics are SiO<sub>2</sub>,

Al<sub>2</sub>O<sub>3</sub>, CaO and/or MgO. Many inorganic wastes are composed of such compounds that can be used as raw materials for glass-ceramic production <sup>1,2)</sup>. Some of the various wastes used as raw materials are coal ash <sup>3)</sup>, metallurgical slags <sup>4-6)</sup>, waste glass <sup>7)</sup>, fly ash <sup>8, 9)</sup>, and electric arc furnace slag <sup>10)</sup>. The utilization of these wastes as raw materials has two advantages, i.e. the plentiful constituent stabilization of such wastes (such as Pb and Cd) in a glassy matrix and their low prices as raw materials.

The more important practical problem of such waste-derived glasses is controlling the crystallization step due to their chemical composition complexity <sup>2)</sup>. The main aspect in crystallization of waste-derived glasses is their low potential for bulk nucleation. As a result, bulk crystal nucleation is a prerequisite for a successful glass-ceramic production route. Therefore, understanding nucleation stage is necessary <sup>1)</sup>. For bulk crystallization of such glasses, nucleating agents such as sulfides, transition metal oxides (such as Cr<sub>2</sub>O<sub>3</sub>, iron oxides, TiO<sub>2</sub>), fluorides, and P<sub>2</sub>O<sub>5</sub> can be used <sup>11-13)</sup>.

The previous studies in glass-ceramic productions from iron and steel production wastes were mainly focused on the blast furnace slag. The aim of this

\* Corresponding Author

Tel: + 98 81 38411460, Fax: +98 81 38380520

Email: samad.ghasemi@hut.ac.ir

Address: Department of Metallurgy and Materials Engineering, Hamedan University of Technology, Hamedan 65155- 579, Iran

1. Assistant Professor

2. Professor

study is to utilize different iron and steel production wastes including the blast furnace flow dust, converter slag, converter sludge, and agglomeration sludge for glass-ceramic productions.

## 2. Materials and Methods

The mixtures of iron and steel making wastes of a steel plant were used as raw materials in this study. The 10 kg batch for glassmaking was prepared using 18% the blast furnace slag, 9% the blast furnace flow dust, 4.5% converter slag, 12% converter sludge, 7% agglomeration sludge, 30% silica sand, 12% fluorine and 7% sodium carbonate. The chemical compositions (wt. %) of each raw material was determined by X-ray fluorescence (XRF, Bruker, S4pioneer, Germany) analysis in which the results are shown in Table 1. As can be seen in Table 1, the major chemical components of the blast furnace slag are silica and lime, whereas for the blast furnace flow dust, converter sludge and agglomeration sludge, the major components are iron oxides. Also, there is a noticeable amount of residual carbon in the composition of the blast furnace flow dust and agglomeration sludge. Silica sand was added to the composition in order to improve glass formation ability while cooling the melt. Fluorine and sodium carbonate were added as fluxes to decrease the melting temperature and making the glass melt homogeneously in a short melting time.

After dry grinding and milling, the mixture of raw materials was transferred to a silicon carbide crucible and melted at 1400 °C for 1hr in an oil fuel fire furnace. In order to have more homogeneity, the melt was stirred mechanically several times while melting. The resultant glass melt was poured in 1×2×5 cm<sup>3</sup> steel molds which were preheated at 400 °C. The samples then immediately were transferred to a 500 °C electric furnace to avoid thermal shocks that

can have an impact on the mechanical properties of solid samples. After 1 hr annealing at 500 °C, the samples were furnace cooled to the room temperature.

To investigate crystallization behavior of the glass, differential thermal analysis (DTA) was conducted in Al<sub>2</sub>O<sub>3</sub> pans and heated in dynamic air atmosphere up to 1400 °C at a rate of 10 °C/min. The DTA experiment was conducted using a NETZSCH STA429, Germany, by heating 50 mg glass powder (120- 180 μm). For the sake of investigation the crystallization process on isothermal conditions, two glass samples were heat treated by the following schedules. The first sample, GC1, heated at 700 °C for 1 hr and the second sample, GC2, heated at 700 °C for 1hr for nucleation, and then heat treated at 850 °C for 1hr, for the growth of ceramic phases. Both samples were then cooled in furnace to room temperature. X-ray diffraction (XRD) method was used to identify crystalline phases formed in the glass during heating. A XL-30 Philips diffractometer (40 kV) with Cu K<sub>α</sub> radiation (λ = 0.15406 nm) was used for XRD measurements.

The XRD patterns were recorded in the 2θ range of 20–70 degree (step size 0.05 °, time per step 1 sec). The microstructure glass and glass-ceramic samples were investigated by a Philips XL30 scanning electron microscopy (SEM) equipped with EDAX.

To reveal the microstructure in SEM investigations, the samples were first etched in 5% HF acid for 10s and then coated with gold film.

The micro-hardness of each phase was determined by a Vickers' indenter at 200g load and dwell time of 15s. Ten indentations were made on each sample to obtain an average value of hardness. The three-point flexural strength of the glass and glass ceramics were also measured at room temperature by using specimens according to ASTM C158 at a cross-head speed of 2 mm/min.

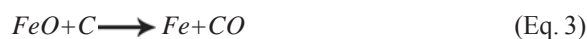
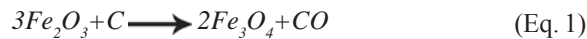
Table 1. Chemical composition (wt. %) of the raw materials.

	SiO <sub>2</sub>	CaO	MgO	Al <sub>2</sub> O <sub>3</sub>	FeO	Fe <sub>2</sub> O <sub>3</sub>	TiO <sub>2</sub>	K <sub>2</sub> O	Na <sub>2</sub> O	PbO	ZnO	L.O.I
Blast Furnace Slag	36.4	35.41	8.85	9.6	1.11	0	3.14	0.81	0.4	0	0.012	0
Blast Furnace Dust	10	5.36	1.81	1.86	10.5	36.37	0	0.42	0.31	0.15	0.3	32
Converter Slag	14.6	45.22	4.85	3.92	7.41	12	1.08	0.11	0.31	0.01	0.012	0
Converter Sludge	1.53	6.3	1.7	0.65	11.8	71.21	0.28	0.52	0.27	0.08	0.024	3.5
Agglomeration Sludge	10.41	12.23	3.76	3.06	5.8	28.66	0.78	0.45	0.27	1	1.32	30.4

### 3. Results and Discussion

#### 3.1. Melting

Table 2 shows the chemical analysis of the batch before melting (theoretical composition, calculated regarding the percentages and chemical compositions of the original raw materials extracted from Table 1) and the chemical composition of the as-cast glass (after melting). It can be seen from this table that some compositional changes occurred after melting, especially, decreasing the total content of iron oxides. It indicates a relative increase in the  $Fe^{+2}/Fe^{+3}$  ratios in as-cast glass to that ratio in the batch before melting. Also some iron was completely reduced and settled at the bottom of the crucible as iron melted. The increased  $Fe^{+2}/Fe^{+3}$  ratio and complete reduction of some iron oxides can be explained through the reaction reduction between iron oxides and residual carbon in the raw materials (especially in the blast furnace flow dust and agglomeration sludge) as the following Eqs. :



#### 3.2. Crystallization and thermal properties

Fig. 1 shows the DTA profile of the glass which determines the glass characteristics such as the transition temperature, crystallization temperature, and thermal behavior of the glass. It can be seen that softening point ( $T_s$ ) is 570 °C and also, two crystallization peaks ( $T_p$ ) at 730 °C and 805 °C are observed. The softening point of the glass is lower than the similar ones. Also it should be noted that the viscosity of the glasses can be reduced by making their chemical compositions more complex, probably through making new eutectic temperatures<sup>14)</sup>. In addition, endothermic peaks observing at 1010 °C and 1250 °C in the sample are attributed to the melting of different phases in the sample. Thus, the crystallization temperature of the samples was determined regarding the exothermic peaks of crystallization. therefore, the

first sample, GC1, heated at 700 °C for 1hr and the second one, GC2, heated at 850 °C for 1hr.

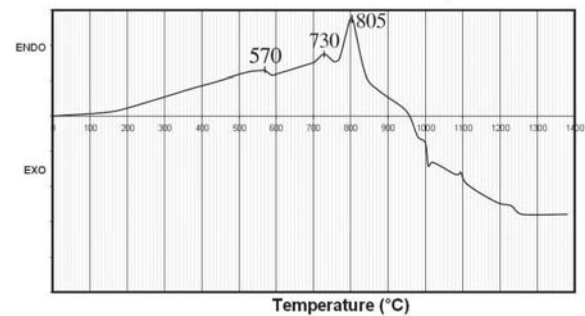


Fig. 1. Differential Thermal Analysis (DTA) diagram of the base glass.

Fig. 2 shows the XRD pattern for the base glass and GC1 and GC2 glass-ceramic samples. The pattern shows that the base glass is almost completely amorphous. The diffraction pattern of GC1 sample is analogous to the base glass, indicating that no detectable ceramic phase created during heating at 700 °C. After soaking at 850 °C, the GC2 sample, the crystallization has been already started and the main formed crystalline phase was diopside,  $Ca(Fe,Mg)Si_2O_6$ .

Fig. 3a and Fig. 3b show the SEM general view of the GC1 and GC2 glass ceramic samples respectively. The microstructures are taken using SEM, through backscatter electrons (BSE) on the polished and etched surface. Both figures show some recognizable spherical bright particles in the glass matrix.

These isolated crystals dispersed in the glass matrix. A magnified photograph of the sphere-shaped crystals is shown in Fig. 4a. EDAX analysis confirmed that the bright regions are metallic iron particles (Fig. 4b). These metallic iron particles are the products of carbothermic reduction of the iron oxides. The in situ produced iron particles are finely dispersed in the glass structure while melting process and trapped in the solid glass matrix during the rapid cooling. Pennyk et al.<sup>15)</sup> showed that it takes a long time for such iron micro-droplets to settle. Fig. 3a and Fig. 3b show the SEM general view of the GC1 and GC2 glass ceramic samples respectively.

Table 2. Chemical compositions of the employed formulation (wt. %) before and after melting.

Composition (%)	SiO <sub>2</sub>	CaO	MgO	Al <sub>2</sub> O <sub>3</sub>	FeO	Fe <sub>2</sub> O <sub>3</sub>	TiO <sub>2</sub>	K <sub>2</sub> O	Na <sub>2</sub> O	PbO	ZnO	CaF <sub>2</sub>	LOI
Before melting	51.49	10.50	1.40	1.08	3.37	12.41	0.28	0.11	4.20	0.07	0.08	10	4.92
After melting	53.2	12.1	3.4	3.08	10.53	0.96	1.5	0.35	4.2	0.02	0.09	10.3	0

The microstructures are taken using SEM, through backscatter electrons (BSE) on the polished and etched surface. Both figures show some recognizable spherical bright particles in the glass matrix. These isolated crystals dispersed in the glass matrix. A magnified photograph of the sphere-shaped crystals is shown in Fig. 4a. EDAX analysis confirmed that the bright regions are metallic iron particles (Fig. 4b). These metallic iron particles are the products of carbothermic reduction of the iron oxides. The in situ produced iron particles are finely dispersed in the glass structure while melting process and trapped in the solid glass matrix during the rapid cooling. Pennyk et al.<sup>15)</sup> showed that it takes a long time for such iron micro-droplets to settle.

Therefore, considering the XRD and EDS, it can be understood that the crystallization process is influenced by the heterogeneous bulk nucleation on pre-existing metallic iron micro-particles.

The mismatch between the coefficients of the thermal expansion of the metal and glass, high interfacial energy and thus, high strain which presents at the particle-glass interface, make these sites the favorable nucleating sites<sup>11, 12)</sup>. The presence of metallic iron in the glass matrix greatly enhances crystallization volume by means of the formation of uniform fine grained ceramic microstructure. In addition, by image analyzing of Fig. 3a and 3b, it can be seen that the number of crystallized ceramic

grains in the GC2 sample (i.e.  $1410 \pm 53 \text{ mm}^2$ , Fig. 3b) is relatively equal to the number of iron micro-particles in the GC1 sample (i.e.  $1418 \pm 53 \text{ mm}^2$ , Fig. 3a). Therefore, the nucleation mechanism of the studied glass is heterogeneous bulk nucleation on the preexisting metallic iron micro-particles.

### 3.3. Mechanical properties

Table 3 shows the results of the flexural strength and Vickers microhardness measurements of the base glass, GC1 and GC2 glass-ceramics. It can be seen that the crystallization of the glass improves bending strength, while it has no considerable effect on Vickers microhardness.

The Crystallization produces a material having greater flexural strength than that of the base glass.

The glass flexural strength was  $52.7 \pm 5 \text{ MPa}$ , while the partially crystallized sample, GC2, had a flexural strength of  $88.3 \pm 5 \text{ MPa}$ , a notable increase of 167%. The increase in flexural strength by the crystallization is in agreement with other reported values<sup>16,17)</sup>.

It can be concluded that the improvement of the flexural strength by incorporating ceramic particles may be attributed to the homogeneous distribution of the ceramic phase in the matrix. In addition the density of the glass ceramic samples was a little higher than the base glass (Table 3).

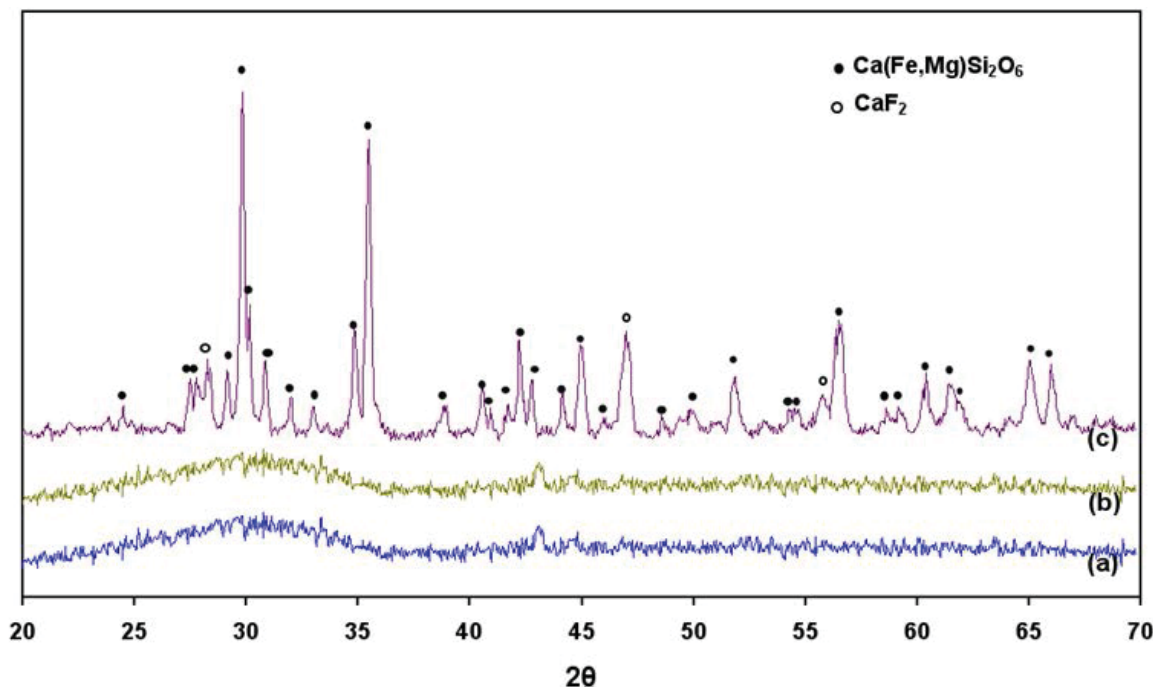


Fig. 2. XRD pattern of (a) base glass, (b) after heating at 700 °C for 1 hr (GC1) and (c) after heating at 850 °C for 1 hr (GC2).

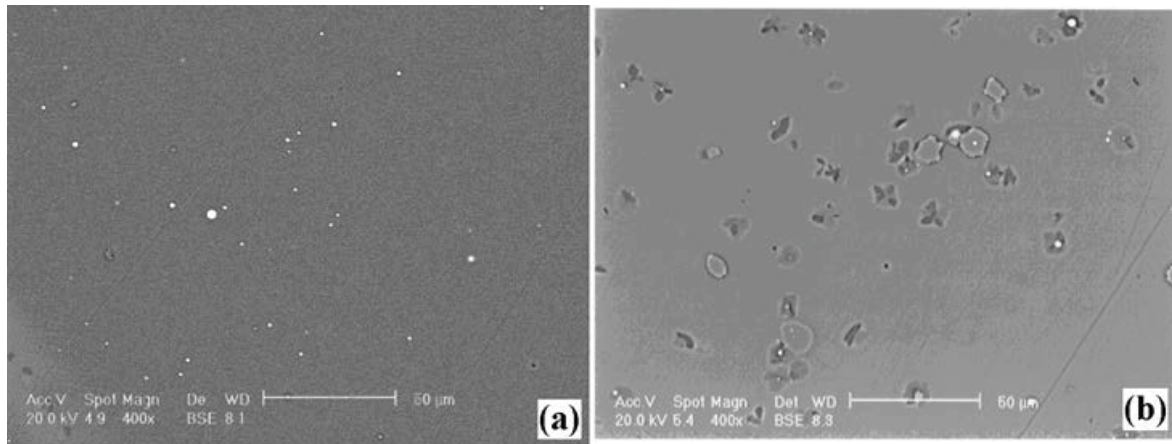


Fig. 3. The SEM micrograph of glass samples heat treated: (a) 700 °C for 1 hr (GC1) and (b) 850 °C for 1 hr (GC2).

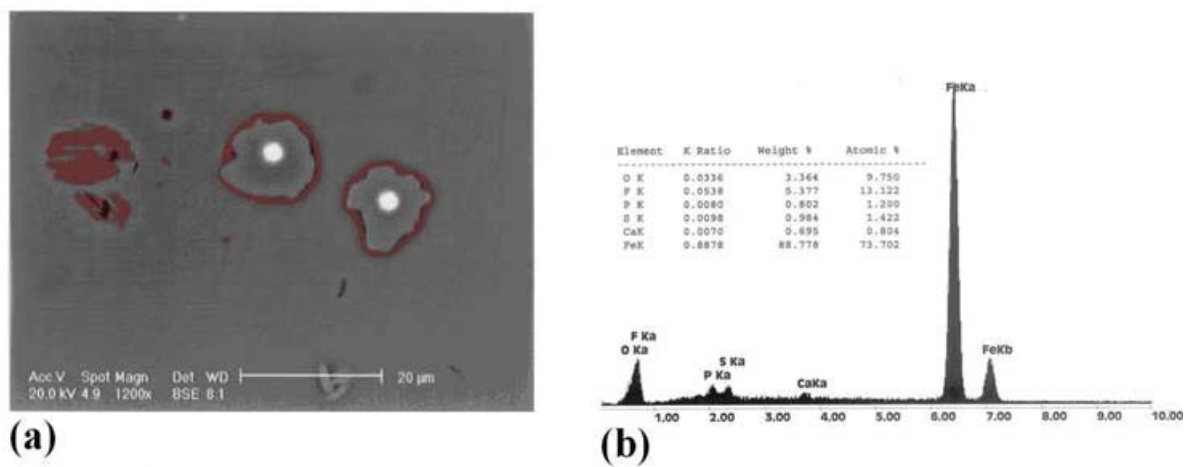


Fig. 4. (a) SEM micrograph of GC2 and (b) the EDAX spectra of the bright particle at the ceramic phase center.

Table 2. Chemical compositions of the employed formulation (wt. %) before and after melting.

	Vickers microhardness	Flexural Strength (MPa)	Density (gr/cm <sup>3</sup> )
Base Glass	753± 18	52.7± 5	2.57± 0.02
GC1	768± 21	59.2± 5	2.63± 0.02
GC2	824± 21	88.3± 5	2.74± 0.02

#### 4. Conclusions

This study showed that various iron and steel making wastes can be recycled and converted to glass bodies and then according to the crystallization treatment converted to glass-ceramics. This process is recognized as an acceptable economic and environmental solution to such wastes. The major result of this research was the formation of diopside ceramic phases on fixed number of pre-existing iron microparticles. These iron particles are those dispersed

in the glass melt as a result of reduction reaction between iron oxides and residual carbon presented in the raw materials.

As a result of the presence of such iron nuclei, the bulk crystallized glass-ceramic with less than 10 µm diameter ceramic phases have been produced without using nucleating agents. The production of glass ceramic using metallurgical wastes and subsequent crystallization lead to homogeneous dispersion of ceramic phases in the glass matrix and improving the properties.

## References

- [1] W. Holand and G. H. Beall: *Glass- Ceramic Technology*, John Willey & Sons, New Jersey, (2012).
- [2] R. D. Rawlings, J.P. Wu and A. R. Boccaccini: *J. Mater. Sci.*, 41(2006), 733.
- [3] C. Leroy, M.C. Ferro, R. C. C. Monteiro and M. H. V. Fernandes: *J. Eur. Ceram. Soc.*, 21(2001), 195.
- [4] B. Lin, H. Wang, X. Zhu, Q. Liao and B. Ding: *Appl. Therm. Eng.*, 96(2016) 432.
- [5] E. M. M. Ewais, G. Grathwohl and Y. M. Z. Ahmed: *J. Am. Ceram. Soc.*, 93(2010) 671.
- [6] K. Das, S. Raha, D. Chakraborty, B. and Sk. Saheb Ali: *Trans. Ind. Ceram. Soc.*, 71(2012), 137.
- [7] W. Yi Zhang, H. Gao and Y. Xu: *J. Eur. Ceram. Soc.*, 31(2011), 1669.
- [8] I. Kourti and C.R. Cheeseman: *Resour. Conserv. Recy.*, 54(2010) 769.
- [9] L. Han-qiao, W. Guo-xia, L. Yin and D. Fei- ying: *J. Cent. South. Univ. Technol.*, 18(2011), 1945.
- [10] A. Kamusheva, E. M. A. Hamzawy and A. Karmanov: *J. Chem. Techn. Metal.*, 50(2015), 512.
- [11] M. Rezvani, B. Eftekhari- Yekta, M. Solati-Hashjin and V.K. Marghussian: *Ceram. Int.*, 31(2005), 75.
- [12] G.A. Khate: *Ceram. Int.*, 37(2011), 2193.
- [13] S. Ghosh, A.D. Sharma, A.K. Mukhopadhyay, P. Kundu and R.N. Basu: *Int. J. Hydrogen. Energ.*, 35(2010), 272.
- [14] M.B. Volf: *Technical Approach to Glass, Glass Science and Technology*, Elsevier, (1990).
- [15] P. IWAMASA and R. J. FRUEH: *ISIJ. Int.*, 36(1996), 1319.
- [16] K. Yukimitu, R. C. Oliveira, E. B. Arajo, J. C. S. Moraes and L. H. Avanci: *Thermochim. Acta.*, 426(2005), 157.
- [17] F.C. Serbena, I. Mathias, C.E. Foerster and E.D. Zanotto: *Acta. Mater.*, 86(2015), 216.